Automatica 166 (2024) 111696

Contents lists available at ScienceDirect

Automatica

journal homepage: www.elsevier.com/locate/automatica

A constrained control framework for unmanned aerial vehicles based on Explicit Reference Governor☆

Gaetano Tartaglione [a,*], Marco M. Nicotra [b], Roberto Naldi [c], Emanuele Garone [d]

[a] Dipartimento di Ingegneria, Università degli Studi di Napoli Parthenope, Centro Direzionale 80143 Napoli, Italy
[b] Department of Electrical, Computer, and Energy Engineering, University of Colorado Boulder, 425 UCB, Boulder (CO), USA
[c] Center for Research on Complex Automated Systems, University of Bologna, Viale C. Pepoli 3/2 40136 Bologna, Italy
[d] Department of Control and System Engineering, Université Libre de Bruxelles, Av. F.D. Roosevelt 50, Bruxelles, Belgium

ARTICLE INFO

Article history:
Received 18 February 2022
Received in revised form 25 November 2023
Accepted 5 March 2024
Available online 9 May 2024

Keywords:
Unmanned aerial vehicles
Lyapunov stability
Constrained control
Reference governors

ABSTRACT

This paper tackles the constrained control problem of unmanned aerial vehicles with planar multirotors. The proposed solution splits the constrained control problem into two separate tasks, i.e. stabilization and constraint enforcement. It is shown that the problems addressed by each individual layer is much simpler than the original combined problem. For the unconstrained control of UAVs we consider a control scheme based on a cascade structure. The Lyapunov function for the stabilized cascaded system is then derived. Using this Lyapunov function, we develop an Explicit Reference Governor for constraint enforcement. Numerical simulation shows the effectiveness of the proposed approach.

1. Introduction

Nowadays, the advances in the field of Unmanned Aerial Vehicle (UAV) allow us to use them in an increasing number of applications performing a wide range of tasks, such as search and rescue (Tomic et al., 2012), surveillance (Kingston, Rasmussen, & Humphrey, 2016), transportation (Klausen et al., 2020), precision agriculture and smart farming (Tokekar et al., 2016), and so on. Although the free-flight control of these autonomous systems has been largely investigated, see e.g. Hua et al. (2013) and references therein, the constrained control of UAVs remains quite challenging due to their fast dynamics, strong nonlinearities, and modest on-board computational power. Existing constraint handling strategies can roughly be divided in two categories: optimization-based schemes and closed-form methods.

The idea behind optimization-based schemes is to solve an optimal control problem at each sampling time instant. In this context, the most common approach is Model Predictive Control (MPC), which generates the control input by minimizing a cost function over a receding time horizon (Alexis, Nikolakopoulos, & Tzes, 2012). Since these schemes are confined to a small computational footprint (Malyuta et al., 2022), i.e. flight control is only a small part of all the tasks that an autonomous vehicle must perform, the main drawback of these schemes is the difficulty to implement them in real-time.

An alternative optimization-based scheme is the Reference Governor (RG) approach, which is an *add-on* control unit that ensures constraint satisfaction by manipulating the reference of a pre-stabilized system (Lucia, Franzè, & Sznaier, 2020; Lucia, Sznaier, & Franzè, 2014). The main interest RG schemes is that they usually have lower computational requirements with respect to MPC (Kahveci & Kolmanovsky, 2009). In the last few years, a novel scheme, called Explicit Reference Governor (ERG) , was introduced in the literature. The ERG is a framework inspired by the RG philosophy whose main novelty is that it does not require any online optimization. The main idea behind the ERG is to manipulate the derivative of the applied reference in continuous time using a suitable nonlinear control law that ensures that constraints are satisfied at all time.

The objective of this paper is to propose a systematic framework based on the ERG for enforcing both state and input constraints while maintaining a relatively small computational effort. This will be done using a paradigm inspired by the multi-layer approach known as the Guidance, Navigation, and Control (GNC) architecture. In our framework *Control Layer* is tasked with pre-stabilizing the UAV dynamics without taking constraints into account. The *Navigation Layer* is tasked with enforcing constraint satisfaction by manipulating the reference of the pre-stabilized system. This will be done using the ERG. Finally, it is assumed that at each time instant the *Guidance Layer* provide a single desired set-point for the UAV.

☆ The material in this paper was not presented at any conference. This paper was recommended for publication in revised form by Associate Editor Abdelhamid Tayebi under the direction of Editor Thomas Parisini.

* Corresponding author.
E-mail addresses: gaetano.tartaglione@uniparthenope.it (G. Tartaglione), marco.nicotra@colorado.edu (M.M. Nicotra), roberto.naldi@unibo.it (R. Naldi), emanuele.garone@ulb.be (E. Garone).

https://doi.org/10.1016/j.automatica.2024.111696

The unconstrained control of UAVs is the object of a rich literature, see e.g. Hua et al. (2013) and references therein. The most popular strategy for controlling UAVs consists in using a cascade structure that controls the attitude and the position of the UAV using two separate control loops, taking advantage of a timescale separation between the attitude and the position dynamics (Marconi & Naldi, 2007). Although this control architecture is a well-known solution, to the authors' best knowledge, the existing literature does not provide a Lyapunov function for the resulting closed-loop system. Since the availability of a Lyapunov function for the pre-stabilized UAV is at the basis of the approach proposed in this paper, the first part of the paper will derive an analytical representation of such function. The navigation layer will be based on a version of the ERG, which will take advantage of the invariance of the Lyapunov level sets to develop a suitable Navigation Layer. Preliminary results pertaining to the constrained control of UAV by means of an ERG have been presented in Convens, Merckaert, Vanderborght, and Nicotra (2021), Hermand et al. (2018) and Nicotra, Naldi, and Garone (2016). These results have been obtained by considering conservative assumptions during the design of the ERG, i.e. the inner loop dynamics are assumed sufficiently fast inner to be treated as either ideal or as a bounded external disturbance. Now, for the first time, we can relax the above assumptions by providing a Lyapunov function for the pre-stabilized system.

2. Preliminaries

In this section, we provide a brief summary of quaternion algebra and of the nonlinear dynamic model of an UAV, including some state and input constraints of interest.

Quaternion algebra - Let $\mathbb{H}$ denote the set of quaternions. Any element $h \in \mathbb{H}$ can be expressed as $h = a + ib + jc + kd$, where a, b, c, d are real numbers and i, j, k are imaginary numbers subject to the quaternion group multiplication rules (Shuster, 1993). A vector $u \in \mathbb{R}^3$ is *an unit vector* if $u^T u = 1$. Likewise, a quaternion $q \in \mathbb{H}$ is *an unit quaternion* if $qq^* = 1$, where q^* is the complex conjugate of q. Given $v \in \mathbb{H}$, it is possible to perform a rotation of α radians around a unit vector u by defining the unit quaternion $q = \cos(\alpha/2) + (iu_1 + ju_2 + ku_3)\sin(\alpha/2)$, and computing $v' = q\, v\, q^*$.

The same operation can also be performed in $\mathbb{R}^3$ by computing $v' = R(q)v$, where the $R(q)$ satisfies the Euler–Rodriguez formula

$$R(q) = I_3 + 2q_R q_I^\wedge + 2q_I^\wedge q_I^\wedge, \tag{1}$$

where $q_R = \cos\frac{\alpha}{2} \in \mathbb{R}$ and $q_I = [u_1\ u_2\ u_3]\sin\frac{\alpha}{2} \in \mathbb{R}^3$ are the real and imaginary component of $q \in \mathbb{H}$, respectively, and $\wedge : \mathbb{R}^3 \to \mathbb{R}^{3\times 3}$ denotes the cross-product operator. Additional information about quaternions, including the computation of their time derivative, can be found in Shuster (1993).

UAV dynamic model As detailed in Hua et al. (2013), most Vertical Take-Off and Landing (VTOL) aircraft can be modelled through the following state-space model

$$\begin{cases} m\ddot{p} = mg \cdot e_3 - T \cdot R(q)e_3 \\ \begin{bmatrix}\dot{q}_R \\ \dot{q}_I\end{bmatrix} = \frac{1}{2}E(q)\omega \\ J\dot{\omega} = -\omega^\wedge J\omega + \tau, \end{cases} \tag{2}$$

where $g \approx 9.81\,\mathrm{m/s^2}$ is the gravitational acceleration, $e_3 = [0\ 0\ 1]$, $p \in \mathbb{R}^3$ is the VTOL position (defined in the global reference frame), $q \in \mathbb{H}$ is its attitude (defined as the rigid rotation from the body reference frame to the global reference frame), note that $qq^* = 1$, $\omega \in \mathbb{R}^3$ is its angular velocity (defined in the body reference frame), $R(q)$ is the rotation matrix (1), and $E(q)$ is the differential kinematics matrix

$$E(q) = \begin{bmatrix} -q_I^T \\ q_R I_3 + q_I^\wedge \end{bmatrix}. \tag{3}$$

The generalized control inputs are given in terms of a resulting thrust force $T \in \mathbb{R}$ and torque vector $\tau \in \mathbb{R}^3$, both of which are defined in the body reference frame.[1] The model parameters are the aircraft mass $m \in \mathbb{R};\ m > 0$ and inertia matrix $J \in \mathbb{R}^{3\times 3};\ J = J^T > 0$.

This paper considers a VTOL subject to both actuator saturation and collision avoidance concerns, leading to the following set of state and input constraints

$$T \in [0, T_{\max}], \qquad T_{\max} > mg; \tag{4a}$$
$$\|\tau\| \le \tau_{\max}, \qquad \tau_{\max} > 0; \tag{4b}$$
$$a^T p + b \ge 0, \qquad a \in \mathbb{R}^3,\ b \in \mathbb{R}; \tag{4c}$$
$$\|p - p_0\| \ge c, \qquad p_0 \in \mathbb{R}^3,\ c > 0. \tag{4d}$$

where constraints (4a) and (4b) are introduced to avoid actuators saturations, while constraints (4c) and (4d) are used to model a planar surface and a spherical surface, respectively, that define no-fly zones for the UAV. Note that, while for the sake of simplicity we consider only one constraint in the form (4c) and one in the form (4d), the proposed framework can easily account for multiple constraints in the form (4c) and (4d).

3. Problem statement

Given a reference position $r \in \mathbb{R}^3$ and reference yaw $\phi \in (-\pi, \pi]$, the objective of this paper is to design a stabilizing control law that steers the VTOL to the best steady-state admissible approximation of r while simultaneously enforcing at each time instant the dynamic constraints (4), meaning

$$r^* = \operatorname{argmin}_w \|r - w\|^2, \tag{5a}$$
$$\text{s.t. } a^T w + b \ge 0, \tag{5b}$$
$$\|w - p_0\| \ge c, \tag{5c}$$

where $w \in \mathbb{R}^3$ is an appropriate reference position. This objective is achieved using a multilayered approach that partitions the constrained control problem in two distinct tasks based on the Explicit Reference Governor framework detailed in Nicotra and Garone (2018).

The first task, addressed by the *Control Layer*, is to pre-stabilize the VTOL dynamics to appropriate references $w \in \mathbb{R}^3$ and $\theta \in (-\pi, \pi]$, without taking into account the constraints. The second task, addressed by the *Navigation Layer*, is to manipulate the dynamics of $w(t)$, $\theta(t)$ so that they asymptotically converge to r^*, ϕ while also ensuring that the pre-stabilized system does not violate the constraints (4). The following problem statements formalize the objectives of the control layer and the navigation layer, respectively.

Problem 1 (*Control*)**.** Given the VTOL dynamic model (2), let $x = [p, \dot{p}, q_R, q_I, \omega]$ and $u = [T, \tau]$ be the state and control vectors, respectively. Given a constant reference position $w \in \mathbb{R}^3$ and yaw $\theta \in [-\pi, \pi)$, design a pre-stabilizing feedback law

$$u = h(x, w, \theta), \tag{6}$$

[1] This formulation captures a wide variety of VTOL configurations (e.g. quadrotors, planar multirotors, ducted fans) where the thrust vector belongs to a fixed body axis.

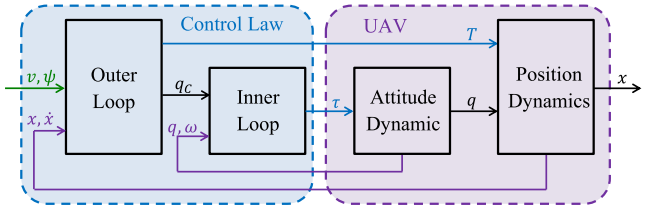

Fig. 1. Representation of the control scheme.

such that the closed-loop system admits

$$\bar{x}_w = \begin{bmatrix} w & 0 & \cos\frac{\theta}{2} & \sin\frac{\theta}{2} & e_3 & 0 \end{bmatrix} \tag{7}$$

as an asymptotically stable equilibrium point. □

Problem 2 (*Navigation*)**.** Given the VTOL dynamic model (2) subject to the pre-stabilizing feedback law (6), determine a reference governor law

$$\dot{w} = h_w(r, \phi, w, \theta), \quad \dot{\theta} = h_\theta(r, \phi, w, \theta), \tag{8}$$

such that, given suitable initial conditions,

1. constraints (4) are always satisfied, for any piece-wise continuous reference $r(t) \in \mathbb{R}^3$ and $\phi(t) \in [-\pi, \pi]$;
2. for any constant reference $r \in \mathbb{R}^3$ and $\phi \in [-\pi, \pi]$, $w(t)$ asymptotically tends to r^* satisfying (5) and $\theta(t)$ asymptotically tends to ϕ. □

4. Control layer

The objective of the control layer is to solve Problem 1 by designing a primary feedback loop that pre-stabilizes the VTOL dynamics. This will be done using the cascade control approach, see e.g. Isidori, Marconi, and Serrani (2003), Marconi and Naldi (2007) and Pflimlin et al. (2006), which consists in stabilizing the VTOL position and attitude using two separate control loops. As illustrated in Fig. 1, the proposed control scheme is based on the idea of introducing the virtual control input $q_C \in \mathbb{H}$; $q_C q_C^* = 1$ and implementing the following steps: (i) Design an *outer loop*, which computes the attitude q_C needed to control the VTOL position; design an *inner loop* to control the VTOL attitude using q_C as a reference; (iii) determine under what conditions the *interconnection* of the two control loops is asymptotically stable.

4.1. Outer loop control

The objective of the outer loop is to control the position of the VTOL so that it asymptotically tends to a constant $v \in \mathbb{R}^3$ under the assumption that the attitude can be used as a control input. Given $q = q_C$, the position dynamics of the state-space model (2) become

$$m\ddot{p} = mg \cdot e_3 - T \cdot R(q_C)e_3, \tag{9}$$

where $-T \cdot R(q_C)e_3$ is the thrust vector expressed in the global reference frame. Since both T and q_C are control inputs, the thrust vector can be assigned as a PD with gravity compensation strategy,

$$T \cdot R(q_C)e_3 = m\left(k_p\,(p - w) + k_d\dot{p} + g \cdot e_3\right), \tag{10}$$

where k_p, k_d are positive scalars. For details on how to compute q_C given Eq. (10) and the yaw reference ϕ, the reader is referred to Appendix A. The following proposition provides a strict Lyapunov function for the resulting closed-loop system.

Proposition 1. *Let system (9) be subject to the control law (10) with k_p, $k_d > 0$. Given a constant reference w, then $\begin{bmatrix} p^T & \dot{p}^T \end{bmatrix}^T = \begin{bmatrix} w^T & 0^T \end{bmatrix}^T$ is a Globally Exponentially Stable (GES) equilibrium point and*

$$V_{Out} = \frac{1}{2}\begin{bmatrix} p - w \\ \dot{p} \end{bmatrix}^T \begin{bmatrix} (k_p + \epsilon k_d^2)I_3 & \epsilon k_d I_3 \\ \epsilon k_d I_3 & I_3 \end{bmatrix} \begin{bmatrix} p - w \\ \dot{p} \end{bmatrix}, \tag{11}$$

is a strict Lyapunov function $\forall \epsilon \in (0, 1)$. □

Proof. Given $\epsilon < 1$, Eq. (11) is a Lyapunov candidate function for the equilibrium point $p = w$ and $\dot{p} = 0$. By taking its time derivative and substituting (9)–(10), it follows that $\dot{V}_{Out} = -\begin{bmatrix} p - w \\ \dot{p} \end{bmatrix}^T \begin{bmatrix} \epsilon k_p k_d I_3 & 0 \\ 0 & (1 - \epsilon)k_d I_3 \end{bmatrix} \begin{bmatrix} p - w \\ \dot{p} \end{bmatrix}$, which is negative definite $\forall \epsilon \in (0, 1)$. ■

4.2. Inner loop control

The objective of the inner loop is to control the attitude of the VTOL under the assumption that the desired control attitude q_C remains constant. Given the attitude error quaternion

$$\tilde{q} = q q_C^*, \tag{12}$$

the attitude dynamics in (2) can be rewritten in error coordinates

$$\begin{cases} \begin{bmatrix} \dot{\tilde{q}}_R \\ \dot{\tilde{q}}_I \end{bmatrix} = \frac{1}{2} E(\tilde{q})\omega \\ J\dot{\omega} = -\omega^\wedge J\omega + \tau, \end{cases} \tag{13}$$

and stabilized using a PD controller in quaternion space

$$\tau = -h_p \tilde{q}_I - h_d \omega, \tag{14}$$

where h_p, h_d are positive scalars. The following proposition provides a strict Lyapunov function for the resulting closed-loop system.

Proposition 2. *Let system (13) be subject to the control law (14) with h_p, $h_d > 0$. Then, $[\tilde{q}_R\ \tilde{q}_I\ \omega] = [1\ 0\ 0]$ is an exponentially stable equilibrium point and*

$$V_{In} = 2h_p(1 - \tilde{q}_R) + \frac{1}{2}\begin{bmatrix} \tilde{q}_I \\ \omega \end{bmatrix}^T \begin{bmatrix} 4\eta h_d I_3 & 2\eta J \\ 2\eta J & J \end{bmatrix} \begin{bmatrix} \tilde{q}_I \\ \omega \end{bmatrix}, \tag{15}$$

is a strict Lyapunov function $\forall \eta \in (0, \bar{\eta})$, where $\bar{\eta} = \min\{h_d/(\mu(J) + h_d/2h_p)\ ,\ h_d/\lambda_3\{J\}\}$, $\mu(J) = \lambda_3\{J\}\cos\operatorname{atan}\frac{\Delta\lambda\{J\}}{\lambda_3\{J\}} + \Delta\lambda\{J\}\sin\operatorname{atan}\frac{\Delta\lambda\{J\}}{\lambda_3\{J\}}$, $\Delta\lambda\{J\} = \lambda_3\{J\} - \lambda_1\{J\}$, and $\lambda_1\{J\}$, $\lambda_3\{J\}$ are equal to the smallest and largest eigenvalue of the inertia matrix J, respectively. □

Proof. Given $\eta < h_d/\lambda_3\{J\}$, Eq. (15) is a Lyapunov candidate function for the equilibrium point $\tilde{q}_R = 1$, $\tilde{q}_I = 0$, and $\omega = 0$. By taking its time derivative and substituting[2] (13)–(14), it follows that $\dot{V}_{In} = -\begin{bmatrix} \tilde{q}_I \\ \omega \end{bmatrix}^T \begin{bmatrix} 2\eta h_p I_3 & \eta h_d(\tilde{q}_R - 1)I_3 \\ \eta h_d(\tilde{q}_R - 1)I_3 & h_d I_3 - \eta J(\tilde{q}_R I_3 - \tilde{q}_I^\wedge) \end{bmatrix} \begin{bmatrix} \tilde{q}_I \\ \omega \end{bmatrix}$. By taking into account the modulus of $\tilde{q}_I$ and ω, $\dot{V}_{In}$ can be upper-bounded as

$$\dot{V}_{In} \le -\begin{bmatrix} \sin\frac{|\tilde{\alpha}|}{2} \\ \|\omega\| \end{bmatrix}^T Q_{In}(\tilde{\alpha}) \begin{bmatrix} \sin\frac{|\tilde{\alpha}|}{2} \\ \|\omega\| \end{bmatrix}, \tag{16}$$

[2] Performing this step requires the use of the properties $a \times (a \cdot b) = 0$ and $a \cdot (b \times c) = c \cdot (a \times b)$, $\forall a, b, c \in \mathbb{R}^3$, where $\times$ and $\cdot$ are the vector and scalar products, respectively.

where $Q_{In}(\tilde{\alpha})$ is equal to

$$\begin{bmatrix} 2\eta h_p & \eta h_d\left(\cos\frac{|\tilde{\alpha}|}{2}-1\right) \\ \eta h_d\left(\cos\frac{|\tilde{\alpha}|}{2}-1\right) & h_d-\eta\left(\lambda_3\{J\}\cos\frac{|\tilde{\alpha}|}{2}+\Delta\lambda\{J\}\frac{\sin|\tilde{\alpha}|}{2}\right)\end{bmatrix}.$$

Since $\lambda_3\{J\}\cos\frac{|\tilde{\alpha}|}{2}+\Delta\lambda\{J\}\sin\frac{|\tilde{\alpha}|}{2}\leq\mu(J)$ and $\cos\frac{|\tilde{\alpha}|}{2}\geq 0$, $\forall\tilde{\alpha}\in[-\pi,\pi]$, it follows that $Q_{In}(\tilde{\alpha})>\bar{Q}_{In}$, where

$$\bar{Q}_{In}=\begin{bmatrix}2\eta h_p & \eta h_d \\ \eta h_d & h_d-\eta\mu(J)\end{bmatrix} \tag{17}$$

is positive definite $\forall\eta\in(0,h_d/(\mu(J)+h_d/2h_p))$]. ■

4.3. Interconnection

The objective of this section is to show under what conditions the proposed cascade control structure ensures asymptotic stability. Although this has already been addressed in the literature by leveraging the classic Small Gain Theorem (Jiang, Teel, & Praly, 1994), existing results, e.g. Isidori et al. (2003), Marconi and Naldi (2007) and Pflimlin et al. (2006), limit themselves with implying the *existence* of a Lyapunov function. To the authors' best knowledge, existing literature does not actually provide a closed-form Lyapunov function for underactuated VTOLs (Ryll, Bülthoff, & Giordano, 2015). By taking advantage of the Lyapunov-based Small Gain Theorem developed in Jiang, Mareels, and Wang (1996), this paper performs an in-depth stability analysis that proposes the formulation of a Lyapunov function for the interconnected system. This result is stated in the following theorem.

Theorem 1. *Let system (2) be subject to the control laws (10), (14) with $k_p>0$, $k_d>0$, $h_p>0$ and $h_d\propto\sqrt{h_p}$. Then, given a constant reference position $w\in\mathbb{R}^3$ and yaw angle $\theta\in[-\pi,\pi)$, the equilibrium point (7) is asymptotically stable for sufficiently large h_p. Moreover,*

$$V=\max\{V_{Out}\ ,\ \chi_{Out}(\varphi_{In}(V_{In}))\} \tag{18}$$

is a Lyapunov function for all initial conditions such that $V(0)\leq\chi_{Out}(\Delta\alpha)$, where $\Delta\alpha$ is subject to the restriction

$$0<\Delta\alpha<\arccos\left(\frac{b-\sqrt{b^2-ac}}{a}\right), \tag{19}$$

where $a=(k_p-\epsilon k_d^2)^2$, $b=k_p^2+2\epsilon k_p k_d^2(1-\epsilon)+\epsilon^2k_d^4$, and $c=(k_p+\epsilon k_d^2)^2$, V_{Out} and V_{In} are given in (11) and (15),

$$\varphi_{In}(V_{In})=2\arccos\left(1-\frac{V_{In}}{2(h_p+\eta(h_d-\eta\lambda_3\{J\}))}\right), \tag{20}$$

and

$$\chi_{Out}(\|\tilde{\alpha}\|_\infty)=\max_{\sigma\in[0,d]}\begin{bmatrix}\sigma\\ \mu(\sigma)\end{bmatrix}^T\begin{bmatrix}W^TPW & W^TPM\\ M^TPW & M^TPM\end{bmatrix}\begin{bmatrix}\sigma\\ \mu(\sigma)\end{bmatrix}, \tag{21}$$

with

$$d=(1-c_\alpha)g \tag{22}$$

$$\mu(\sigma)=\operatorname{sgn}\left(W^TPM\right)\sqrt{\sigma(d-\sigma)\frac{W^TW}{M^TM}} \tag{23}$$

$$P=\frac{1}{2}\sqrt{Q_{Out}}^{-T}\begin{bmatrix}(k_p+\epsilon k_d^2) & \epsilon k_d\\ \epsilon k_d & 1\end{bmatrix}\sqrt{Q_{Out}}^{-1}, \tag{24}$$

$$W=\sqrt{Q_{Out}}^{-T}\begin{bmatrix}\epsilon k_d\\ 1\end{bmatrix}, \tag{25}$$

$$M=\operatorname{Ker}(W^T), \tag{26}$$

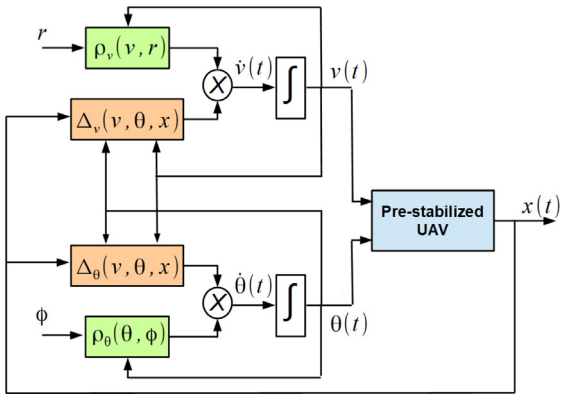

Fig. 2. Schematic representation of the ERG for the control of a VTOL.

$$Q_{Out}=\frac{1}{2}\begin{bmatrix}2\epsilon k_p k_d\, c_\alpha & (k_p+\epsilon k_d^2)(c_\alpha-1)\\ (k_p+\epsilon k_d^2)(c_\alpha-1) & 2k_d(c_\alpha-\epsilon)\end{bmatrix}, \tag{27}$$

$$c_\alpha=\cos\|\tilde{\alpha}\|_\infty\ . \tag{28}$$

Proof. See Appendix B.

Note that the restriction (19) must be verified at each time instant so that the stability analysis holds. Accordingly, from now restriction (19) will be considered in the sets of constraints to be satisfied at all time, together with (4). This result is a necessary stepping stone for the following section, which will leverage the Lyapunov level-sets to enforce the system constraints.

5. Navigation layer

It is now possible to address Problem 2 by implementing an Explicit Reference Governor. The ERG is based on two fundamental components: the *Dynamic Safety Margin* and the *Navigation Field* (Nicotra & Garone, 2018). A schematic representation of the ERG is illustrated in Fig. 2.

The dynamic safety margins $\Delta_w(x,w)$ and $\Delta_\theta(x,\theta)$ represent distances between the constraints and the system trajectory that would emanate from the state x given the constant references w and θ. The navigation fields $\rho_w(w,r)$ and $\rho_\theta(\theta,\phi)$ represent the directions along the path that lead from the current references w and θ to the desired references r and ϕ remaining strictly inside the constraints. The ERG framework solves Problem 2 by manipulating the applied references as follows

$$\dot{w}(t)=\Delta_w(w,\theta,x)\rho_w(w,r), \tag{29a}$$

$$\dot{\theta}(t)=\Delta_\theta(w,\theta,x)\rho_\theta(\theta,\phi). \tag{29b}$$

Intuitively, Eqs. (29) imply that the dynamic safety margins regulate the modulus of $\dot{w}(t)$ and $\dot{\theta}(t)$, and hence their values indicate how safe it is to change the applied references without risking a constraint violation, while the navigation field determines the direction of $\dot{w}(t)$ and $\dot{\theta}(t)$. In order to compute the dynamic safety margins and the attractions fields in (29), we can separately exploit the contributions of the constraints (4) and (19).

In particular, for the computation of the dynamic safety margins, we consider that

$$\Delta_w(w,\theta,x)=\min\{\Delta_\alpha^w(w,\theta,x),\Delta_\tau(w,\theta,x),\Delta_T(w,x),\Delta_{wall}(w,x),\Delta_{obs}(w,x)\}, \tag{30a}$$

$$\Delta_\theta(w,\theta,x)=\min\{\Delta_\alpha^\theta(w,\theta,x),\Delta_\tau(w,\theta,x)\}, \tag{30b}$$

where Δ_α^w and Δ_α^θ are the dynamic safety margins associated to the restriction on the attitude error (19), Δ_T^w is the dynamic safety

margins associated to the constraint on the maximum thrust (4a), Δ_τ is the dynamic safety margins associated to the constraint on the maximum torque (4b), Δ^w_{wall} is the dynamic safety margins associated to the constraint of the wall avoidance (4c), and Δ^w_{obs} is the dynamic safety margins associated to the constraint of the obstacle avoidance (4d).

For what concerns the navigation field, we can define

$$\rho_w(w\,,r) = \frac{r-w}{\max\left(\|r-w\|\,,\eta_w\right)} + \rho^w_{wall}(w\,,r) + \rho^w_{obs}(w\,,r)\,, \tag{31a}$$

$$\rho_\theta(\theta,\phi) = \frac{\phi-\theta}{\max\left(|\phi-\theta|\,,\eta_\theta\right)}\,, \tag{31b}$$

where $\frac{r-w}{\max(\|r-w\|,\eta_v)}$ and $\frac{\phi-\theta}{\max(|\phi-\theta|,\eta_\theta)}$ are generic attraction terms, $\eta_w > 0$ $\eta_\theta > 0$ are two scalar tuning parameters, ρ^w_{wall} is a repulsion field associated to the constraint of the wall avoidance (4c), and ρ^w_{obs} is the repulsion field associated to the constraint of the obstacle avoidance (4d). Notice that not all constraints generate a repulsion field, as certain constraints (e.g. maximum torque constraints) do not introduce any limitation on the admissible set-points.

In the following paragraphs we address one by one the construction of suitable dynamic safety margins and navigation fields.

Maximum Attitude Error - The limit on the attitude error $|\tilde\alpha| \le \Delta\alpha$ ensures that (18) is a strict Lyapunov function and is fundamental for ensuring asymptotic stability and enforcing all the other constraints. For this kind of constraints it is convenient to implement a Lyapunov-based dynamic safety margin (see Nicotra and Garone (2018) for more details). To do so, it is necessary to identify a threshold value associated to the constraint $|\tilde\alpha| \le \Delta\alpha$. The following proposition shows a way to construct a dynamic safety margin for this constraint.

Proposition 3. *Given the Lyapunov function (18) and given $\Delta\alpha$ satisfying (19), the threshold value*

$$\Gamma_{\Delta\alpha} = \chi_{Out}(\Delta\alpha) \tag{32}$$

is such that $V(p,\dot p,q_R,q_I,\omega,w,\phi) \le \Gamma_{\Delta\alpha}$ ensures $|\tilde\alpha| \le \Delta\alpha$. □

Proof. The statement follows directly from the proof of Theorem 1 since $V(\tau) \le \chi_{Out}(\Delta\alpha)$ implies $|\tilde\alpha| \le \varphi_{In}(V_{In}(t)) \le \Delta\alpha$, $\forall t \ge \tau$. ■

Since the threshold value $\Gamma_{\Delta\alpha}$ does not depend on the current reference, it can be computed off-line and stored in memory. Furthermore, since $r \in \mathbb{R}^3$ and $\phi \in [-\pi,\pi)$ represent a position and an angle, respectively, it is reasonable to assume that $\dot w$ and $\dot\theta$ will have a significantly different effect on the system dynamics. Hence, we decouple the two references based on their effect on the Lyapunov function. In particular, $\dot w$ has a direct influence on $V_{Out}(p,\dot p,w)$, whereas $\dot\theta$ has a direct influence on $V_{In}(\tilde q_R,\tilde q_I,\omega)$. Due to the interactions between V_{Out} and V_{In}, however, $\dot w$ and $\dot\theta$ will also present an indirect influence on V_{In} and V_{Out}, respectively. To account for this problem, we consider

$$\Delta^w_\alpha(w\,,\theta\,,x) = \kappa_w\left(\Gamma_{\Delta\alpha} - V_{Out}(p,\dot p,w)\right) \min\left(\frac{\Delta\alpha - \varphi_{In}(V_{In}(\tilde q_R,\tilde q_I,\omega))}{\Delta\Gamma_{In}},1\right), \tag{33}$$

$$\Delta^\theta_\alpha(w\,,\theta,x) = \kappa_\theta\left(\Delta\alpha - \varphi_{In}(V_{In}(\tilde q_R,\tilde q_I,\omega))\right) \min\left(\frac{\Gamma_{\Delta\alpha} - V_{Out}(p,\dot p,w)}{\Delta\Gamma_{Out}},1\right), \tag{34}$$

where $\kappa_w\,,\kappa_\theta\,,\Delta\Gamma_{In}$ and $\Delta\Gamma_{Out}$ are positive scalars. Definitions (33) and (34) of the dynamic safety margins ensure that $\dot w$ and $\dot\theta$ will behave independently as long as $\Delta\alpha - \phi_{In}(V_{In}(\tilde q_R,\tilde q_I,\omega)) > \Delta\Gamma_{In}$ and $\Gamma_{\Delta\alpha} - V_{Out}(p,\dot p,w) > \Delta\Gamma_{Out}$. However, the two references will be coupled as soon as one of the two loops is in proximity of a constraint violation.

For what concerns the navigation field, since at steady state this constraint is always satisfied, so it does not introduce any repulsive barrier.

Maximum Torque - In this section, we show how to use an invariance-based approach to design a Dynamic Safety Margin able to enforce the torque saturation constraints $\|\tau\| \le \tau_{\max}$. The following lemma provides a starting point for the proposed approach.

Lemma 1. *Given the inner loop controller (14) and the Lyapunov function (15), let Γ_τ be the solution to the optimization problem*

$$\begin{cases} \min\ V_{In}(\tilde q,\tilde\omega), \quad \text{s.t.} \\ h_p^2\,\tilde q_I^T\tilde q_I + h_d^2\,\omega^T\omega - \tau^2_{\max} = 0, \\ \begin{bmatrix} 0 \\ h_p\tilde q_I \\ h_d\omega \end{bmatrix}^T \begin{bmatrix} \frac{1}{2}E(\tilde q)\omega \\ J^{-1}(-\omega^\wedge J\omega - h_p\tilde q_I - h_d\omega) \end{bmatrix} \ge 0, \end{cases} \tag{35}$$

Then, $\{(\tilde q,\omega) \mid c(\tilde q,\omega) \le 0\} \cap \{(\tilde q,\omega) \mid V_{In}(\tilde q,\omega) \le \Gamma_\tau\}$, with $c(\tilde q,\omega) = h_p^2\tilde q_I^T\tilde q_I + h_d^2\omega^T\omega - \tau^2_{\max}$, is a positively invariant set. □

Proof. The invariance of $\{(\tilde q,\omega) \mid V_{In}(\tilde q,\omega) \le \Gamma_\tau\}$ follows directly from the fact that (15) is a Lyapunov function. As detailed in Blanchini (1999), the constraint boundary of the set $\{(\tilde q,\omega) \mid c(\tilde q,\omega) \le 0\}$ is locally positively invariant if the system dynamics point in a non-increasing direction of $c(\tilde q,\omega)$, meaning if

$$\nabla c(\tilde q,\omega)^T \begin{bmatrix} \dot{\tilde q} \\ \dot\omega \end{bmatrix} \le 0. \tag{36}$$

It then follows from the definition of Γ_τ that the boundary of the constraint set is locally positively invariant $\forall(\tilde q,\omega):\ V_{In}(\tilde q,\omega) \le \Gamma_\tau$, which concludes the proof. ■

Note that (35) is lower-bounded by the largest Lyapunov level-set contained in $\{(\tilde q,\omega) \mid c(\tilde q,\omega) \le 0\}$. This is sufficient to ensure $\Gamma_\tau > 0$. At this point, since the value of the inner loop Lyapunov function is effectively limited by the maximum attitude error $\Delta\alpha$ enforced in the previous section, it is possible to ensure $V_{In}(\tilde q,\omega) \le \Gamma_\tau$ by complementing (19) with the additional restriction

$$0 < \Delta\alpha < \varphi_{In}(\Gamma_\tau), \tag{37}$$

with φ_{In} given in (20). Doing so enables us to assign the dynamic safety margin associated to the maximum torque constraint as

$$\Delta_\tau(p,\dot p,q_R,q_I,\omega,w,\theta) = \kappa_\tau(\tau_{\max} - \|\tau\|), \tag{38}$$

with $\kappa_\tau > 0$. Note that, typically, (19) is more restrictive than (37).

In analogy to the attitude error constraint, the steady-state torques $\tau = 0$ are always smaller than $\tau_{\max} > 0$. Thus all steady-state configurations of the UAV satisfy constraints. As such, this constraint does not need any repulsion term in the overall navigation field (31).

Maximum Thrust - This section addresses the input saturation constraint $T \le T_{\max}$, which is not linear in the state variables since $T = m\left\|k_p(p-w) + k_d\dot p + ge_3\right\|$. A possible approach to tackle this constraint is to make a distinction between the steady-state thrust mge_3 and the dynamic feedback $mk_p(p-w) + mk_d\dot p$. This can be done by taking advantage of the triangular inequality

$$T \le \left\|mk_p(p-w) + mk_d\dot p\right\| + mg.$$

To enforce the maximum thrust constraint, it is therefore sufficient to ensure

$$\left\| k_p(p-w) + k_d\dot{p} \right\| \leq \frac{T_{\max} - mg}{m}, \tag{39}$$

which can be rewritten as the quadratic constraint

$$\begin{bmatrix} p-w \\ \dot{p} \end{bmatrix}^T \begin{bmatrix} k_p^2 I_3 & k_p k_d I_3 \\ k_p k_d I_3 & k_d^2 I_3 \end{bmatrix} \begin{bmatrix} p-w \\ \dot{p} \end{bmatrix} \leq \left(\frac{T_{\max} - mg}{m} \right)^2. \tag{40}$$

As discussed in Section 4.1, the outer loop can be modelled as a linear system subject to a bounded[3] time-varying uncertainty $|\tilde{\alpha}| \leq \Delta\alpha$. As a result, the Lyapunov-based dynamic safety margin can be applied by finding a common Lyapunov function for all the possible perturbations of the outer loop dynamics. An option is to use the outer loop Lyapunov function (11)

$$V_T(p, \dot{p}, w) = \begin{bmatrix} p-w \\ \dot{p} \end{bmatrix}^T P_T \begin{bmatrix} p-w \\ \dot{p} \end{bmatrix}, \tag{41}$$

with $P_T > 0$. Following from Eq. (B.1), the common Lyapunov function must satisfy the Lyapunov equation

$$\begin{bmatrix} 0 & I_3 \\ k_p R(\tilde{q}) & k_d R(\tilde{q}) \end{bmatrix}^T P_T + P_T \begin{bmatrix} 0 & I_3 \\ k_p R(\tilde{q}) & k_d R(\tilde{q}) \end{bmatrix} \leq 0,$$

for all $\tilde{q} \in \mathbb{H}$ such that $2\arccos(\tilde{q}_R) \leq \Delta\alpha$. By taking advantage of the rotational symmetry of the system, by defining

$$P_T = \begin{bmatrix} \hat{P}_{T,11} I_3 & \hat{P}_{T,12} I_3 \\ \hat{P}_{T,21} I_3 & \hat{P}_{T,22} I_3 \end{bmatrix},$$

and by introducing the 2×2 matrices

$$\hat{P}_T = \begin{bmatrix} \hat{P}_{T,11} & \hat{P}_{T,12} \\ \hat{P}_{T,21} & \hat{P}_{T,22} \end{bmatrix}, \hat{K}_T = \begin{bmatrix} k_p^2 & k_p k_d \\ k_p k_d & k_d^2 \end{bmatrix},$$

a convenient Lyapunov function can be obtained as a solution of the following optimization problem, similarly to what done in Garone, Nicotra, and Ntogramatzidis (2018)

$$\begin{cases} \min \log\det(\hat{P}_T), \quad \text{s.t.} \\ A(0)^T \hat{P}_T + \hat{P}_T A(0) \leq 0; \\ A(\Delta\alpha)^T \hat{P}_T + \hat{P}_T A(\Delta\alpha) \leq 0; \\ \hat{P}_T \geq \hat{K}_T, \end{cases} \tag{42}$$

where

$$A(\tilde{\alpha}) = \begin{bmatrix} 0 & 1 \\ k_p \cos(\tilde{\alpha}) & k_d \cos(\tilde{\alpha}) \end{bmatrix}. \tag{43}$$

Note that $\hat{K}_T$ is a dyadic matrix that can be written as $\hat{K}_T = c_T c_T^T$ with $c_T = [k_p \; k_d]$ and given the quadratic Lyapunov function (41) computed solving (42) we can compute the threshold value as proposed in Nicotra and Garone (2018)

$$\Gamma_T = \frac{(T_{\max} - mg)^2}{m^2 c_T^T \hat{P}_T^{-1} c_T}, \tag{44}$$

from which we obtain the dynamic safety margin related to the input saturation

$$\Delta_T(p, \dot{p}, w) = \kappa_T \left(\Gamma_T - V_T(p, \dot{p}, w) \right), \tag{45}$$

where κ_T is a positive constant. It can be noted that the Eqs. (42) define a convex optimization problem that can be computed off-line and that does not depend on the reference. Similarly, the value of Γ_T in (44) does not depend of the current reference. Accordingly, both the Lyapunov matrix P_T and the threshold value Γ_T can be computed off-line and stored in memory.

As for the previous two cases, this constraint does not introduce any repulsion term in the navigation field (31).

Wall Avoidance - Note that the wall constraint $c^T p + d \geq 0$ only takes into account outer loop variables. Hence, the dynamic safety margin can be computed by treating the outer loop as a linear system with a bounded time-varying uncertainty $|\tilde{\alpha}| \leq \Delta\alpha$. As a result, the following Lyapunov function is proposed

$$V_W(p, \dot{p}, w) = \begin{bmatrix} p-w \\ \dot{p} \end{bmatrix}^T P_W \begin{bmatrix} p-w \\ \dot{p} \end{bmatrix}, \tag{46}$$

where $P_W = \begin{bmatrix} \hat{P}_{W,11} I_3 & \hat{P}_{W,12} I_3 \\ \hat{P}_{W,21} I_3 & \hat{P}_{W,22} I_3 \end{bmatrix}$, and $\hat{P}_W > 0$ is the solution to

$$\begin{cases} \min \log\det(\hat{P}_W), \quad \text{s.t.} \\ A(0)^T \hat{P}_W + \hat{P}_W A(0) \leq 0, \\ A(\Delta\alpha)^T \hat{P}_W + \hat{P}_W A(\Delta\alpha) \leq 0, \\ \hat{P}_W \geq c_W c_W^T, \end{cases} \tag{47}$$

with $A(\tilde{\alpha})$ given in (43) and $c_W = \begin{bmatrix} 1 & 0 \end{bmatrix}^T$. Since the solution of the optimization problem (47) provides a Lyapunov function which is specifically designed for limiting the maximum position error $\|p - w\|$, the threshold value associated to a wall constraint $c^T p + d \geq 0$ is

$$\Gamma_W(w) = \frac{(c^T w + d)^2}{c_W^T \hat{P}_W^{-1} c_W}, \tag{48}$$

from which, we obtain

$$\Delta_{wall}(p, \dot{p}, w) = \kappa_{wall} \left(\Gamma_W(w) - V_W(p, \dot{p}, w) \right), \tag{49}$$

where κ_{wall} is a positive constant.

Unlike the previous constraints addressed in this Section, the wall constraint $c^T p + d \geq 0$ can potentially be violated at steady-state $p = w$. As a result, the attraction term in (31a) is no longer sufficient to ensure the correct behaviour of the ERG. Since the domain $\mathcal{D} = \{w : c^T w + d \geq 0\}$ is convex, a suitable choice[4] for computing the repulsion field (31a) can be

$$\rho^w_{wall}(w, r) = \max\left(\frac{\zeta - (c^T w + d)}{\zeta - \delta}, 0 \right) c, \tag{50}$$

where $\zeta > \delta$ is the influence region of the wall constraint and $\delta > 0$ is the static safety margin.

Obstacle Avoidance - The obstacle avoidance constraint $\|p - p_0\| - R \geq 0$ defines a non-convex admissible region. Given a fixed reference v, it can be shown using triangular inequalities that $\|p - p_0\| \geq \|p_0 - w\| - \|p - w\|$. As a result, $\|p - p_0\| - R \geq 0$ can be enforced by simply ensuring

$$\frac{(p_0 - w)^T}{\|p_0 - w\|}(p - w) \leq R - \|p_0 - w\|. \tag{51}$$

The main interest in Eq. (51) is that it defines a reference-dependent virtual wall $c(w)^T p + d(w) \leq 0$ that guarantees the non-violation of the obstacle. The dynamic safety margin of the previous subsection can therefore be used by choosing $c(w) = \frac{(p_0-w)^T}{\|p_0-w\|}$ and $d(w) = \|p_0 - w\| - \frac{(p_0-w)^T}{\|p_0-w\|} w - R$. In this way, we define $\Gamma_{obs}(w) = \frac{(c(w)^T v + d(w))^2}{c_W^T \hat{P}_W^{-1} c_W}$, from which, we obtain

$$\Delta_{obs}(p, \dot{p}, w) = \kappa_{obs} \left(\Gamma_{obs}(w) - V_T(p, \dot{p}, w) \right), \tag{52}$$

[3] The bound on $\tilde{\alpha}$ is ensured by the presence of the ERG and of the bound on the maximum attitude error.

[4] Eq. (50) assumes that $\|c\| = 1$. Otherwise, the wall constraint should be rescaled as $\hat{c} = c/\|c\|$ and $\hat{d} = d/\|c\|$.

where κ_{obs} is a positive constant.

For what concerns the navigation field, it is worth noting that the domain

$$\mathcal{D} = \{w : c^T + d \geq \delta\} \cup \{w : \|w - p_0\| - R \geq \delta\}$$

contains a spherical hole and as such the navigation field cannot be continuous. Following the approach proposed in Nicotra and Garone (2018), the repulsion field in (31a) can be computed as

$$\rho^w_{obs}(w, r) = \max\left\{\frac{\zeta - (\|p_0 - w\| - R)}{\zeta - \delta}, 0\right\} \cdot \left(\frac{(p_0 - w)^T}{\|p_0 - w\|} + \tilde{\rho}_O(w)\right), \tag{53}$$

with

$$\tilde{\rho}_O(w) = \hat{\text{sgn}}\left(\rho^T_{w,W}(w, r)(p_0 - w)^\perp\right)(p_0 - w)^\perp. \tag{54}$$

Remark 1. Since $(p_0 - w) \in \mathbb{R}^3$, it is worth noting that the perpendicular vector $(p_0 - w)^\perp$ is not uniquely defined. A possible strategy consists in defining

$$(p_0 - w)^\perp = a\,\text{Ker}_1(p_0 - w)^T + \sqrt{1 - a^2}\,\text{Ker}_2(p_0 - w)^T, \tag{55}$$

where Ker_i for $i = 1, 2$ represents the ith column vector of the kernel and $a \in [0, 1]$ can be selected randomly.[5] □

Main Result - The following theorem summarizes the properties of the proposed control law augmented with the proposed explicit reference governor.

Theorem 2. *Let a VTOL aircraft modelled by system (2) and subject to the constraints (4) controlled with the control law (10) and (14), with $k_p > 0$, $k_d > 0$, $h_p > 0$ and $h_d \propto \sqrt{h_p}$ whose reference is managed by (29) with navigation layer subject to the dynamic safety margins (30), whose components are (33), (34), (38), (45), (49) and (52), and navigation fields (31), whose components are (50) and (53). Then any initial condition such that the auxiliary reference position $w(0) \in \mathbb{R}^3$ and yaw angle reference $\theta(0) \in [-\pi, \pi)$ are such that the*

$$\Delta_w(w, \theta, x) \geq 0, \tag{56a}$$

$$\Delta_\theta(w, \theta, x) \geq 0. \tag{56b}$$

and if the influence regions of the obstacle constraints do not overlap with each other and the influence regions of the wall constraints, the following propositions hold

1. *constraints (4) are always satisfied, for any piece-wise continuous reference $r(t) \in \mathbb{R}^3$ and $\phi(t) \in [-\pi, \pi]$;*
2. *for any constant reference $r \in \mathbb{R}^3$ and $\phi \in [-\pi, \pi]$, $w(t)$ asymptotically tends to r^* satisfying (5) and $\theta(t)$ asymptotically tends to ϕ.* □

Proof. From Theorem 1 we obtain that the closed loop system (2), (10) and (14) is asymptotically stable for all references and states that verify $\arccos \tilde{q}_R \leq 2\Delta\alpha$.

By construction, dynamic safety margins (30) satisfy the requirements of Nicotra and Garone (2018, Definition 1), moreover $\Delta_w(w, \theta, x) \geq 0$ and $\Delta_\theta(w, \theta, x) \geq 0$ are sufficient to verify the restriction (19) with the additional constraint (37), and hence to avoid the input saturation (4). Moreover, it can be noted that the navigation fields (31) satisfy the requirements of Nicotra and Garone (2018, Definition 2) by construction. Finally, by considering the hypothesis (56) on the initial condition and the auxiliary reference signals $w(0)$ and $\theta(0)$, all the requirements of Nicotra and Garone (2018, Theorem 1) are satisfied. Hence, the remainder of the proof is therefore a direct result of Nicotra and Garone (2018, Theorem 1). ■

[5] Please note that Eq. (54) is designed to guarantee convergence for whatever choice of $(p_0 - w)^\perp$.

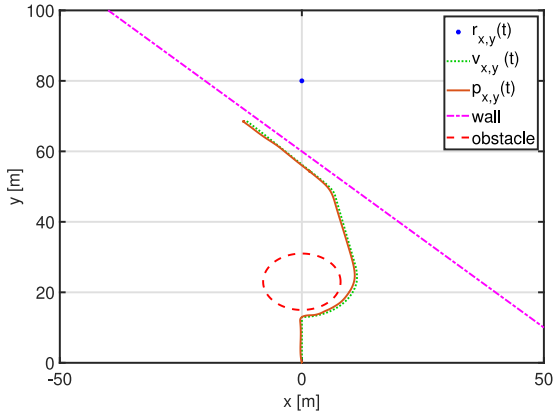

Fig. 3. Planar trajectory performed by the UAV during the flight mission.

6. Numerical validation

In this section we prove the effectiveness of the proposed approach by considering a numerical simulation. We considered the dynamic of a quadrotor characterized by a mass $m = 2$ kg and an inertial matrix $J = diag([0.0082\ \ 0.0082\ \ 0.0164])$ kg m^2. The vehicle moves in a flight environment characterized by a wall, which constraint is defined by $c = [1\ 1\ 0]^T/\sqrt{2}$ and $d = 60/\sqrt{2}$, and a circular obstacle of radius $R = 8$ m and centred in $p_0 = [0\ 23\ 0]^T$ m. The flight mission have been defined by setting the reference position $r = [0\ 80\ 0]^T$ m and the reference yaw $\phi = \pi$, which have to been achieved starting from the initial position $r = [0\ 0\ 0]^T$ m and a null yaw angle. For the control laws (10) and (14), starting from the desired nominal closed-loop dynamics, we have set the following control gains $k_p = 1.0966$, $k_d = 1.4661$, $h_p = 22.4808$ and $h_d = 3.7768$. Fro the navigation layer, we have implemented the procedures described in Section 5, by considering the obstacles in the flight environment the maximum attitude error, and by setting the values $\Delta\alpha = 35$ deg, $\tau_{max} = 0.2$ N m and $T_{max} = 39.24$ N.

Simulation results are summarized in Figs. 3–5. Fig. 3 shows that the flight mission is successfully accomplished by the vehicle. The UAV reaches the best steady-state admissible projection of the desired reference by circumventing the obstacle and by avoiding the wall. Moreover, from data in Fig. 4, it can be noted that also input and state constraints are met during the flight mission due to the applied references. Fig. 5 shows the performance of the cascade control scheme. Moreover, we can note that the navigation layer is able to guarantee the considered input and state constraints, in spite of the control error.

7. Conclusions

In this paper we described the development of a GNC system for the constrained control of an UAV. First we have developed a stabilizing linear control system, based on a cascade architecture for which we identified a Lyapunov function. Using this characterization we developed a navigation layer which enforces the constraints by manipulating the reference of the pre-stabilized system based on an ERG. A numerical validations of the overall scheme has been provided.

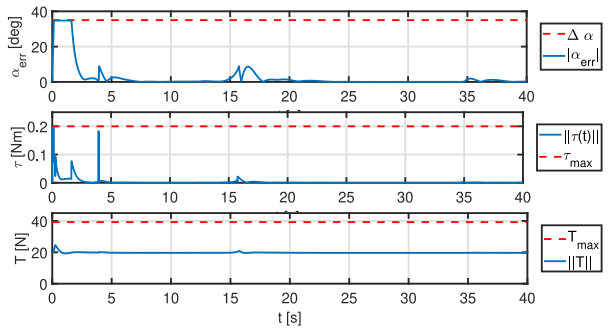

Fig. 4. Evaluation of state and input constraints.

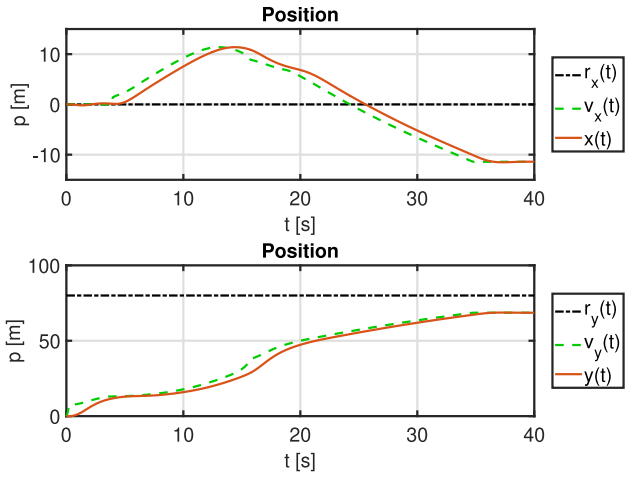

Fig. 5. Performance of outer loop controller.

Appendix A. Thrust Vectoring

Given the outer control law (10), it is necessary to determine a suitable thrust T and control attitude q_C, which provide the desired thrust vector. To this end, consider the components of the desired thrust vector

$$\begin{bmatrix} F_x \\ F_y \\ F_z \end{bmatrix} = -mk_p \begin{bmatrix} p_x - v_x \\ p_y - v_y \\ p_z - v_z \end{bmatrix} - mk_d \begin{bmatrix} \dot{p}_x \\ \dot{p}_y \\ \dot{p}_z \end{bmatrix} - mg \begin{bmatrix} 0 \\ 0 \\ 1 \end{bmatrix}.$$

Since $\|R(q_C)e_3\| = 1$, $\forall q_C \in \mathbb{H}$, the required thrust can be obtained directly from the modulus

$$T = \sqrt{F_x^2 + F_y^2 + F_z^2}. \tag{A.1}$$

As for q_C, it is useful to define $\beta \in [-\pi, \pi]$ as the angle between the axis e_3 and the vector $T \cdot R(q_C)e_3$, i.e.

$$\beta = \arctan \frac{\sqrt{F_x^2 + F_y^2}}{F_z}.$$

The minimum rotation between e_3 and $R(q_C)e_3$ is therefore given by the unitary quaternion q_β, with[6]

$$q_{\beta,R} = \cos\frac{\beta}{2}, \qquad q_{\beta,I} = \frac{\sin\frac{\beta}{2}}{\sqrt{F_x^2 + F_y^2}} \begin{bmatrix} F_y \\ -F_x \\ 0 \end{bmatrix}.$$

[6] Please note that the solution is well-posed even if $F_x^2 + F_y^2 = 0$. Indeed, in this case it follows that $\beta = 0$, which implies $q_{\beta,R} = 1$ and $q_{\beta,I} = 0$.

Although q_β is such that $R(q_C)e_3 = R(q_\beta)e_3$, this property does not imply $q_C = q_\beta$. Indeed, given the unitary quaternion q_θ, with

$$q_{\theta,R} = \cos\frac{\theta}{2}, \qquad q_{\theta,I} = \sin\frac{\theta}{2} e_3,$$

it follows that $e_3 = R(q_\theta)e_3$. The control quaternion q_C can thus be obtained as the combination of an arbitrary rotation θ around the yaw axis e_3 and the minimum rotation β that aligns e_3 with the desired thrust vector. This is given by the quaternion-space product $q_C = q_\beta q_\theta$, which can be computed in matrix form

$$\begin{bmatrix} q_{C,R} \\ q_{C,I} \end{bmatrix} = \begin{bmatrix} q_{\beta,R} & -q_{\beta,I}^T \\ q_{\beta,I} & q_{\beta,R} I_3 + q_{\beta,I}^\wedge \end{bmatrix} \begin{bmatrix} q_{\theta,R} \\ q_{\theta,I} \end{bmatrix}.$$

by taking advantage of the quaternion group multiplication rules (Mishchenko & Solovyov, 2000).

Appendix B. Proof of Theorem 1

The proof of Theorem 1 is based on four lemmas which are provided hereafter. The first two lemmas characterize the input-to-state gains of the outer and inner loops.

To characterize the outer loop behaviour in the presence of a non-zero attitude error $\tilde{q} = qq_C^*$, consider the VTOL model (2). Given $q = \tilde{q}q_C$, the position dynamics can be rewritten as $m\ddot{p} = mg \cdot e_3 - T \cdot R(\tilde{q})R(q_C)e_3$. By substituting the control law (10), the closed-loop system becomes

$$\ddot{p} = -k_p R(\tilde{q})(p - w) - k_d R(\tilde{q})\dot{p} + g(I_3 - R(\tilde{q}))e_3. \tag{B.1}$$

The following lemma extends the results of Proposition 1 by characterizing the ISS properties of the outer loop in the presence of an attitude error.

Lemma 2. *Let system (B.1), with $k_p, k_d > 0$, be subject to a constant applied reference v and a bounded attitude error $\|\tilde{\alpha}\|_\infty \leq \Delta\alpha$ satisfying (19). Then, the Lyapunov function in Eq. (11) satisfies the asymptotic gain $V_{Out} \leq \chi_{Out}(\|\tilde{\alpha}\|_\infty)$, defined by (21).* □

Proof. Given $\epsilon < 1$, (11) is an ISS-Lyapunov candidate function. By taking its time derivative and substituting (B.1), it follows that

$$\begin{aligned} \dot{V}_{Out} = &-\frac{1}{2}\begin{bmatrix} p - w \\ \dot{p} \end{bmatrix}^T \begin{bmatrix} \mathcal{Q}_{11} & \mathcal{Q}_{21}^T \\ \mathcal{Q}_{21} & \mathcal{Q}_{22} \end{bmatrix} \begin{bmatrix} p - w \\ \dot{p} \end{bmatrix} \\ &+ \begin{bmatrix} p - w \\ \dot{p} \end{bmatrix}^T \begin{bmatrix} \epsilon k_d I_3 \\ I_3 \end{bmatrix} g(I_3 - R(\tilde{q}))e_3, \end{aligned} \tag{B.2}$$

where $\mathcal{Q}_{11} = \epsilon k_p k_d (R(\tilde{q})^T + R(\tilde{q}))$, $\mathcal{Q}_{22} = k_d(R(\tilde{q})^T + R(\tilde{q}) - 2\epsilon I_3)$, $\mathcal{Q}_{21} = k_p(R(\tilde{q}) - I_3) + \epsilon k_d^2 (R(\tilde{q})^T - I_3)$.

Using the modulus of $p - w$ and $\dot{p}$, Eq. (B.2) can be upper bounded by

$$\dot{V}_{Out} \leq -\begin{bmatrix} \|p - w\| \\ \|\dot{p}\| \end{bmatrix}^T Q_{Out} \begin{bmatrix} \|p - w\| \\ \|\dot{p}\| \end{bmatrix} + \begin{bmatrix} \|p - w\| \\ \|\dot{p}\| \end{bmatrix}^T \begin{bmatrix} \epsilon k_d \\ 1 \end{bmatrix} d, \tag{B.3}$$

with $Q_{Out} = Q_{Out}(\|\tilde{\alpha}\|_\infty)$ and $d = d(\|\tilde{\alpha}\|_\infty)$ given in Eqs. (27) and (22), respectively. To prove ISS, it is sufficient to note that restriction (19) is such that $Q_{Out}(\|\tilde{\alpha}\|_\infty) > 0$, $\forall \|\tilde{\alpha}\|_\infty \leq \Delta\alpha$. The asymptotic gain can now be computed by finding $\chi_{Out}(\|\tilde{\alpha}\|_\infty)$ such that $V_{Out} \geq \chi_{Out}(\|\tilde{\alpha}\|_\infty)$ implies $\dot{V}_{Out} \leq 0$. To do so, consider the change of coordinates $\zeta = \sqrt{Q_{Out}} \; [\, \|p - w\| \;\; \|\dot{p}\| \,]^T$. Using (25), Eq. (B.3) can be rewritten as

$$\dot{V}_{Out} \leq -\zeta^T\zeta + \zeta^T W d. \tag{B.4}$$

Since W and M in Eqs. (25)–(26) describe an orthonormal basis, the vector ζ can be decomposed into

$$\zeta = \sigma W + \mu M. \tag{B.5}$$

As a result, (B.4) becomes $\dot{V} \leq -\mu^2 M^T M - \sigma(\sigma - d) W^T W$, which is non-negative for $\sigma \in [0, d]$ and

$$\mu \in \left[\sqrt{\sigma(d-\sigma)\frac{W^T W}{M^T M}}\ ,\ \sqrt{\sigma(d-\sigma)\frac{W^T W}{M^T M}} \right].$$

At this point, consider the Lyapunov function (11). By substituting (B.5), it follows that

$$V_{Out} = \begin{bmatrix} \sigma \\ \mu \end{bmatrix}^T \begin{bmatrix} W^T P W & W^T P M \\ M^T P W & M^T P M \end{bmatrix} \begin{bmatrix} \sigma \\ \mu \end{bmatrix}.$$

To end the proof, it is sufficient to note that (21) is the largest value of V_{Out} such that $\dot{V}_{Out}$ is non-negative. ■

It is worth noting that the scalar parameter $\epsilon \in (0, 1)$ in the Lyapunov function (11) can be chosen freely and can be used to maximize the upper bound on $\Delta\alpha$. Given $k_d = 2\zeta\sqrt{k_p}$, where $\zeta > 0$ is the damping ratio of the outer loop, the coefficients of inequality (19) become $a = (1 - 4\zeta^2\epsilon)^2$, $b = 1 + 8\zeta^2\epsilon(1-\epsilon) + 16\zeta^4\epsilon^2$ and $c = (1 + 4\zeta^2\epsilon)^2$. This implies that the bound on $\Delta\alpha$ is independent from k_p. Given a fixed value of the damping ratio,[7] it is possible to maximize the restriction (19) by solving $\max_{\epsilon\in(0,1)} \arccos\left(\frac{b+\sqrt{b^2+ac}}{a}\right)$, which is a convex scalar optimization problem that can be solved off-line. Moreover, given suitable parameters k_p, k_d, ϵ, the optimization problem (21) is the maximization of a smooth scalar function $V_{Out}(\sigma)$ in a bounded interval $\sigma \in [0, d(\|\tilde{\alpha}\|_\infty)]$. In particular, the upper bound $\chi_{Out}(\|\tilde{\alpha}\|_\infty)$ can be easily be computed off-line and stored in a one-dimensional lookup table.

To characterize the inner loop behaviour in the presence of a time-varying control attitude $\dot{q}_C$, consider the following modification to the attitude error dynamics (13)

$$\begin{cases} \begin{bmatrix} \dot{\tilde{q}}_R \\ \dot{\tilde{q}}_I \end{bmatrix} = \frac{1}{2} E(\tilde{q})(\omega - \omega_C) \\ J\dot{\omega} = -\omega^\wedge J\omega + \tau, \end{cases} \tag{B.6}$$

where ω_C is the angular velocity of the control attitude. The following lemma extends the results of Proposition 2 by characterizing the ISS properties of the inner loop

Lemma 3. *Let system (B.6) be subject to the control law (14) with $h_p, h_d > 0$. Then, there exists an asymptotic gain χ_{In} such that $V_{In} \geq \chi_{In}(\|\omega_C\|_\infty)$ implies $\dot{V}_{In} \leq 0$. Moreover, given $\eta \propto h_d$ and $h_d \propto \sqrt{h_p}$, the asymptotic gain χ_{In} remains bounded for arbitrarily large h_p.* □

Proof. Given $\eta < h_d/\lambda_3\{J\}$, (15) is an ISS-Lyapunov candidate function. By taking its time derivative and substituting (B.6), it follows that

$$\dot{V}_{In} = -\begin{bmatrix} \tilde{q}_I \\ \omega \end{bmatrix}^T \begin{bmatrix} 2\eta h_p I_3 & \Sigma \\ \Sigma & h_d I_3 - \eta J(\tilde{q}_R I_3 - \tilde{q}_I^\wedge) \end{bmatrix} \begin{bmatrix} \tilde{q}_I \\ \omega \end{bmatrix} - \begin{bmatrix} \tilde{q}_I \\ \omega \end{bmatrix}^T \begin{bmatrix} \left(h_p + 2\eta\tilde{q}_R h_d\right) I_3 \\ \eta J\left(\tilde{q}_R I_3 + \tilde{q}_I^\wedge\right) \end{bmatrix} \omega_C,$$

where $\Sigma = \eta h_d(\tilde{q}_R - 1) I_3$. In analogy to the proof of Proposition 2, the following upper-bounded is obtained $\dot{V}_{In} \leq -\begin{bmatrix} \sin\frac{|\tilde{\alpha}|}{2} \\ \|\omega\| \end{bmatrix}^T \bar{Q}_{In} \begin{bmatrix} \sin\frac{|\tilde{\alpha}|}{2} \\ \|\omega\| \end{bmatrix} + \begin{bmatrix} \sin\frac{|\tilde{\alpha}|}{2} \\ \|\omega\| \end{bmatrix}^T \bar{D}_{In} \|\omega_C\|_\infty$, with $\bar{Q}_{In}$ given in (17) and $\bar{D}_{In} = \begin{bmatrix} h_p + 2\eta h_d \\ \eta\mu(J) \end{bmatrix}^T$. This is sufficient to prove ISS since $\bar{Q}_{In} > 0$ under the assumption $\eta \in (0, h_d/(\mu(J) + h_d/2h_p))$. To characterize the asymptotic gain, consider the change of coordinates $\zeta = \sqrt{\bar{Q}_{In}} \begin{bmatrix} \sin\frac{|\tilde{\alpha}|}{2} \|\omega\| \end{bmatrix}^T$, and let $\dot{V}_{In} \leq -\zeta^T\zeta + \zeta^T \sqrt{\bar{Q}_{In}}^{-T} \bar{D}_{In} \|\omega_C\|_\infty$, which implies

$$\|\zeta\| \geq \left\| \sqrt{\bar{Q}_{In}}^{-T} \bar{D}_{In} \right\| \|\omega_C\|_\infty \ \Rightarrow\ \dot{V}_{In} \leq 0. \tag{B.7}$$

By upper bounding the Lyapunov function (15) as $V_{In} \leq 2h_p \sin^2\frac{|\tilde{\alpha}|}{2} + \frac{1}{2}\begin{bmatrix} \sin\frac{|\tilde{\alpha}|}{2} \\ \|\omega\| \end{bmatrix}^T \begin{bmatrix} 4\eta h_d & 2\eta\lambda_3\{J\} \\ 2\eta\lambda_3\{J\} & \lambda_3\{J\} \end{bmatrix} \begin{bmatrix} \sin\frac{|\tilde{\alpha}|}{2} \\ \|\omega\| \end{bmatrix}$, and substituting ζ, (B.7) implies $V_{In} \leq \lambda_3\{\hat{Q}\} \|\zeta\|^2$, where

$$\hat{Q} = \frac{1}{2}\sqrt{\bar{Q}_{In}}^{-T} \begin{bmatrix} 4(h_p + \eta h_d) & 2\eta\lambda_3\{J\} \\ 2\eta\lambda_3\{J\} & \lambda_3\{J\} \end{bmatrix} \sqrt{\bar{Q}_{In}}^{-1}. \tag{B.8}$$

As a result, the asymptotic gain is

$$\chi_{In}(\|\omega_C\|_\infty) = \lambda_3\{\hat{Q}\} \left\| \sqrt{\bar{Q}_{In}}^{-T} \bar{D}_{In} \right\|^2 \|\omega_C\|_\infty^2.$$

To study the behaviour of $\chi_{In}(\|\omega_C\|_\infty)$ for increasing h_p, consider $\eta \propto h_d$ and $h_d \propto \sqrt{h_p}$. Given (17), the following proportionalities hold true

$$\bar{Q}_{In} \propto \begin{bmatrix} \sqrt{h_p} h_p & h_p \\ h_p & \sqrt{h_p} \end{bmatrix} \qquad \bar{D}_{In} \propto \begin{bmatrix} h_p \\ \sqrt{h_p} \end{bmatrix}. \tag{B.9}$$

By applying the following property of 2×2 matrices

$$\sqrt{A} = \frac{1}{\sqrt{\mathrm{Tr}(A) + 2\sqrt{\det A}}} \begin{bmatrix} a_{11} + \sqrt{\det A} & a_{12} \\ a_{21} & a_{22} + \sqrt{\det A} \end{bmatrix},$$

it can be shown that $\sqrt{\bar{Q}_{In}}^{-1} \propto \sqrt[4]{h_p} \begin{bmatrix} \frac{1}{h_p} & \frac{1}{h_p} \\ \frac{1}{h_p} & \frac{1}{\sqrt{h_p}} \end{bmatrix}$.

Therefore, given Eqs. (B.8) and (B.9),

$$\sqrt{\bar{Q}_{In}}^{-T} \bar{D}_{In} \propto \sqrt[4]{h_p} \begin{bmatrix} 1 \\ 1 \end{bmatrix}, \qquad \hat{Q} \propto \frac{1}{\sqrt{h_p}} \begin{bmatrix} 1 & 1 \\ 1 & 1 \end{bmatrix}.$$

Since $\chi_{In} \propto \lambda_3\{\hat{Q}\} \left\| \sqrt{\bar{Q}_{In}}^{-T} \bar{D}_{In} \right\|^2 = \frac{\sqrt{h_p}}{\sqrt{h_p}} = 1$, the asymptotic gain $\chi_{In}(\|\omega_C\|_\infty)$ remains bounded for arbitrarily large h_p. ■

Remark 2. The assumption $h_d \propto \sqrt{h_p}$ presented in Lemma 3 is a fairly reasonable design choice. Indeed, for linear systems in the form $\ddot{x} = -h_p x - h_d \dot{x}$, it is customary to assign $h_d = 2\zeta\sqrt{h_p}$ where ζ is the damping ratio and $\sqrt{h_p}$ is the natural frequency. □

Having determined the asymptotic gains between the disturbances and the value of the Lyapunov function, the next step is to characterize the maximum gain between the value of each Lyapunov function and the output of each loop. By using a thrust vectoring technique, the control attitude q_C can be computed directly from the desired outer loop control law (10). Since the inner loop considers the angular velocity ω_C as a disturbance, it is necessary to characterize the maximum gain between the outer loop Lyapunov function V_{Out} and the resulting derivative of the control attitude. This is done in the following lemma.

Lemma 4. *Given the outer loop control law (10), subject to a constant reference position v and yaw angle ϕ, there exists a maximum gain φ_{Out} between the Lyapunov function (11) and the output ω_C. Moreover, $\|\omega_C\|$ is bounded for arbitrarily large values of V_{Out}.* □

[7] The damping ratio ζ is usually chosen during the control design phase based on other considerations.

Proof. Given a constant yaw angle ϕ, the angular velocity ω_C is equal to the derivative of the minimal angle α between the axis e_3 and the vector $T \cdot R(q_C)e_3$, i.e.

$$\alpha = \arctan\left(\frac{1}{F_z}\sqrt{F_x^2 + F_y^2}\right), \tag{B.10}$$

where F_x, F_y and F_z are the components the desired thrust vector. Given Eq. (B.10), it follows that

$$\omega_C = \frac{F_{xy}\dot{F}_z - F_z\dot{F}_{xy}}{F_{xy}^2 + F_z^2}, \tag{B.11}$$

with $F_{xy} = \sqrt{F_x^2 + F_y^2}$. From the outer loop control law (10), we obtain that the derivative of F_z is $\dot{F}_z = mk_pk_d(p_z - w_z) + m(k_d^2 - k_p)\dot{p}_z$, which is proportional to $|p_z - w_z|$ and $|\dot{p}_z|$. Likewise, it can be shown that $\dot{F}_{xy} \propto |p_x - w_x| + |p_y - w_y| + |\dot{p}_x| + |\dot{p}_y|$. Since (11), (B.11) are continuous functions of $p - w$ and $\dot{w}$, there exists a maximum gain φ_{Out} such that $\|\omega_C\| < \varphi_{Out}(V_{Out})$. To prove that $\|\omega_C\|$ is bounded, consider what happens for arbitrarily large V_{Out} and, therefore, for arbitrarily large $\|p - w\|$ and $\|\dot{w}\|$. Given (B.11), it follows that

$$\omega_C \propto \frac{(|p_x - w_x| + |p_y - w_y| + |\dot{p}_x| + |\dot{p}_y|)\cdot(|p_z - w_z| + |\dot{p}_z|)}{|p_x - w_x|^2 + |p_y - w_y|^2 + |p_z - w_z|^2 + |\dot{p}_x|^2 + |\dot{p}_y|^2 + |\dot{p}_z|^2}.$$

As a result, $\|\omega_C\|$ is bounded for any combination of state variables going to infinity. Since it is also continuous, $\varphi_{Out}(V_{Out})$ admits a global maximum. ■

Although Lemma 4 does not explicitly state the gain $\varphi_{Out}(V_{Out})$, its existence and global boundedness will be sufficient for the remainder of this paper. The following lemma will instead provide a more detailed characterization of the maximum gain between the inner loop Lyapunov function and the output $\tilde{\alpha}$.

Lemma 5. *Given the Lyapunov function (15), the output $\tilde{\alpha}$ satisfies the maximum gain $|\tilde{\alpha}| \leq \varphi_{In}(V_{In})$.*

Proof. The Lyapunov function (15) is minimum with respect to the vector ω for $\omega = -2\eta\tilde{q}_I$. By substituting this value in (15), it follows that $V_{In} \geq 2h_p(1 - \tilde{q}_R) + 2\eta\tilde{q}_I^T(h_dI_3 - \eta J)\tilde{q}_I$. By taking into account $\tilde{q}_I^T J\tilde{q}_I^T \leq \lambda_3\{J\}\left\|\tilde{q}_I\right\|^2$ and $\sin^2(x) \geq (1 - \cos(x))$, $\forall x \in [-\pi/2, \pi/2]$, the following lower bound holds true

$$V_{In} \geq 2(h_p + \eta(h_dI_3 - \eta\lambda_3\{J\}))\left(1 - \cos\frac{\tilde{\alpha}}{2}\right), \forall\tilde{\alpha} \in [-\pi, \pi].$$

The statement is then proven by inverting this inequality to obtain (20). ■

Finally, by combining the results presented in the previous lemmas, Theorem 1 can be proven as follows.

Proof (*Theorem 1*)**.** From Lemma 4 we obtain that $\|\omega_C\|_\infty < \varphi_{Out}(V_{Out})$ is bounded regardless of V_{Out}. Additionally, it follows from Lemmas 3 and 5 that the attitude error $\tilde{\alpha}$ will asymptotically satisfy $\|\tilde{\alpha}\| \leq \varphi_{In}(\chi_{In}(\|\omega_C\|_\infty))$, where χ_{In} remains bounded whereas φ_{In} becomes arbitrarily small for arbitrarily large h_p. As a result, there exists a sufficiently large h_p such that $\|\tilde{\alpha}(t)\| \leq \Delta\alpha$, $\forall t \geq \tau$, where $\tau \geq 0$ is a finite time instant. Without loss of generality,[8] consider the case $\tau = 0$. Since the requirements of Lemma 2 hold true, the outer loop will satisfy the asymptotic gain $V_{Out} \leq \chi_{Out}(\|\tilde{\alpha}\|_\infty)$. The stability of the interconnected loops is therefore proven using the Small Gain Theorem since $\chi_{Out}(\varphi_{In}(\chi_{In}(\varphi_{Out}(V_{Out})))) < V_{Out}$ holds true for sufficiently large h_p. As a result, it follows from Jiang et al. (1996) that (18) is a Lyapunov function. To conclude the proof, it is sufficient to note that $V(0) \leq \chi_{Out}(\Delta\alpha)$ implies $\varphi_{In}(V_{In}(t)) \leq \Delta\alpha$, $\forall t \geq 0$. ■

[8] If $\tau > 0$, it is sufficient to define a new timescale $\tilde{t} = t - \tau$ and study the system for $\tilde{t} \geq 0$.

References

Alexis, K., Nikolakopoulos, G., & Tzes, A. (2012). Model predictive quadrotor control: attitude, altitude and position experimental studies. *IET Control Theory & Applications*, *6*(12), 1812–1827.

Blanchini, F. (1999). Set invariance in control. *Automatica*, *35*(11), 1747–1767.

Convens, B., Merckaert, K., Vanderborght, B., & Nicotra, M. M. (2021). Invariant set distributed explicit reference governors for provably safe on-board control of nano-quadrotor swarms. *Frontiers in Robotics and AI*, *8*, 129.

Garone, E., Nicotra, M. M., & Ntogramatzidis, L. (2018). Explicit reference governor for linear systems. *International Journal of Control*, *91*(6), 1415–1430.

Hermand, E., et al. (2018). Constrained control of UAVs in geofencing applications. In *2018 26th mediterranean conference on control and automation* (pp. 217–222).

Hua, M.-D., et al. (2013). Introduction to feedback control of underactuated VTOL vehicles: A review of basic control design ideas and principles. *IEEE Control Systems*, *33*(1), 61–75.

Isidori, A., Marconi, L., & Serrani, A. (2003). Robust nonlinear motion control of a helicopter. *IEEE Transactions on Automatic Control*, *48*(3), 413–426.

Jiang, Z.-P., Mareels, I. M. Y., & Wang, Y. (1996). A Lyapunov formulation of the nonlinear small-gain theorem for interconnected ISS systems. *Automatica*, *32*(8), 1211–1215.

Jiang, Z.-P., Teel, A. R., & Praly, L. (1994). Small-gain theorem for ISS systems and applications. *Mathematics of Control, Signals, and Systems*, *7*(2), 95–120.

Kahveci, N. E., & Kolmanovsky, I. V. (2009). Constrained control of UAVs using adaptive anti-windup compensation and reference governors. SAE Technical Paper.

Kingston, D., Rasmussen, S., & Humphrey, L. (2016). Automated UAV tasks for search and surveillance. In *2016 IEEE conference on control applications* (pp. 1–8).

Klausen, K., et al. (2020). Cooperative control for multirotors transporting an unknown suspended load under environmental disturbances. *IEEE Transactions on Control Systems Technology*, *28*(2), 653–660.

Lucia, W., Franzè, G., & Sznaier, M. (2020). A hybrid command governor scheme for rotary wings unmanned aerial vehicles. *IEEE Transactions on Control Systems Technology*, *28*(2), 361–375.

Lucia, W., Sznaier, M., & Franzè, G. (2014). An obstacle avoidance and motion planning command governor based scheme: The qball-X4 quadrotor case of study. In *53rd IEEE conference on decision and control* (pp. 6135–6140).

Malyuta, D., et al. (2022). Convex optimization for trajectory generation: A tutorial on generating dynamically feasible trajectories reliably and efficiently. *IEEE Control Systems Magazine*, *42*(5), 40–113.

Marconi, L., & Naldi, R. (2007). Robust full degree-of-freedom tracking control of a helicopter. *Automatica*, *43*(11), 1909–1920.

Mishchenko, A., & Solovyov, Y. (2000). Quaternions. *Quantum*, *11*, 4–7.

Nicotra, M. M., & Garone, E. (2018). The explicit reference governor: A general framework for the closed-form control of constrained nonlinear systems. *IEEE Control Systems Magazine*, *38*(4), 89–107.

Nicotra, M. M., Naldi, R., & Garone, E. (2016). A robust explicit reference governor for constrained control of unmanned aerial vehicles. In *Proc. of the American control conference* (pp. 6284–6289).

Pflimlin, J. M., et al. (2006). A hierarchical control strategy for the autonomous navigation of a ducted fan flying robot. In *Proc. of the IEEE international conference on robotics and automation* (pp. 2491–2496).

Ryll, M., Bülthoff, H. H., & Giordano, P. R. (2015). A novel overactuated quadrotor unmanned aerial vehicle: Modeling, control, and experimental validation. *IEEE Transactions on Control Systems Technology*, *23*(2), 540–556.

Shuster, M. D. (1993). A survey of attitude representation. *The Journal of the Astronautical Sciences*, *41*(4), 439–517.

Tokekar, P., et al. (2016). Sensor planning for a symbiotic UAV and UGV system for precision agriculture. *IEEE Transactions on Robotics*, *32*(6), 1498–1511.

Tomic, T., et al. (2012). Toward a fully autonomous UAV: Research platform for indoor and outdoor urban search and rescue. *IEEE Robotics & Automation Magazine*, *19 (Issue: 3)*, 46–56.

Gaetano Tartaglione received the Master's degree in Aerospace Engineering from the second University of Naples, Italy, in 2014 and the Ph.D. degree in Information Engineering from University of Naples "Parthenope", Italy, in 2018. , He is currently an Assistant Professor at the Engineering Department of University of Naples "Parthenope", and his research interests include constrained control of nonlinear systems with applications in nuclear fusion devices and unmanned aerial vehicles, and finite-time stability and stabilization for different class of dynamic systems.

Marco M. Nicotra received his double M.S. degree in mechanical engineering from Politecnico di Milano (Italy) and electromechanical engineering from and Université Libre de Bruxelles (Belgium) in 2012. He received his joint Ph.D. degree from Université Libre de Bruxelles and the University of Bologna (Italy) in 2016. He is currently an Assistant Professor with the Electrical, Computer, and Energy Engineering department of the University of Colorado Boulder (USA). His research interests include constrained control of nonlinear systems with applications in unmanned aerial vehicles, collaborative robotics, and quantum systems.

Roberto Naldi received the B.S and M.S. degrees in Computer Science Engineering from the Alma Mater Studiorum University of Bologna in 2002 and 2004, respectively. In 2008 he got his Ph.D. degree on Automatic Control and Operative Research from the University of Bologna. He is the co-recipient of the 2014 IEEE Control Systems Magazine Outstanding Paper Award for the best paper published on the magazine in the period 2012–2013. His main research interests are nonlinear control and hybrid control systems with application to unmanned aerial vehicles. In 2014 he received an honourable mention for the Young Author Prize of the 19th IFAC World Congress in Cape Town, South Africa.

Emanuele Garone received the Master degree (Laurea) and the Ph.D. degree in systems engineering from the University of Calabria, Rende, Italy, in 2005 and 2009, respectively. Since 2010 he is Professor at the Control Design and System Analysis Department, Université Libre de Bruxelles, Brussels, Belgium. His main research interests focus on constrained control, with a particular emphasis on reference governor schemes. The other main interest of Prof. Garone concerns problems coupling estimation problems with optimization and logistics aspects, including but not limited to optimal sensor selections, optimal planning to collect data, and control over unreliable channels. Prof. Garone is very active in applying the system theoretic approach at large to a large spectrum of real-world applications, ranging to robotics and aeronautics applications, to the control of the fast charge of Li-ion battery, and to exotic applications in epidemiology, agronomy, and entomology.